

Visual Field Abnormalities in Early-Stage Diabetic Retinopathy Assessed by Chromatic Perimetry

J. Jason McAnany,^{1,2} Jason C. Park,¹ and Jennifer I. Lim¹

¹Department of Ophthalmology and Visual Sciences, University of Illinois at Chicago, Chicago, Illinois, United States

²Department of Bioengineering, University of Illinois at Chicago, Chicago, Illinois, United States

Correspondence: J. Jason McAnany, Department of Ophthalmology and Visual Sciences, University of Illinois at Chicago, 1855 W. Taylor St., Chicago, IL 60612, USA; jmcana1@uic.edu.

Received: September 1, 2022

Accepted: January 15, 2023

Published: February 3, 2023

Citation: McAnany JJ, Park JC, Lim JI. Visual field abnormalities in early-stage diabetic retinopathy assessed by chromatic perimetry. *Invest Ophthalmol Vis Sci.* 2023;64(2):8. <https://doi.org/10.1167/iov.64.2.8>

PURPOSE. The purpose of this study was to define the nature and extent of sensitivity loss using chromatic perimetry in diabetics who have mild or no retinopathy.

METHODS. Thirty-four individuals with type II diabetes mellitus who have mild nonproliferative diabetic retinopathy (MDR; $N = 17$) or no diabetic retinopathy (NDR; $N = 17$) and 15 visually normal, non-diabetic controls participated. Sensitivity was assessed along the horizontal visual field meridian using an Octopus 900 perimeter. Measurements were performed under light- and dark-adapted conditions using long-wavelength (red) and short-wavelength (blue) Goldmann III targets. Cumulative defect curves (CDCs) were constructed to determine whether field sensitivity loss was diffuse or localized.

RESULTS. Sensitivity was reduced significantly under light-adapted conditions for both stimulus colors for the NDR (mean defect \pm SEM = -2.1 dB \pm 0.6) and MDR (mean defect \pm SEM = -4.0 dB \pm 0.7) groups. Sensitivity was also reduced under dark-adapted conditions for both stimulus colors for the NDR (mean defect \pm SEM = -1.9 dB \pm 0.7) and MDR (mean defect \pm SEM = -4.5 dB \pm 1.0 dB) groups. For both diabetic groups, field loss tended to be diffuse under light-adapted conditions (up to 6.9 dB loss) and localized under dark-adapted conditions (up to 15.4 dB loss).

CONCLUSIONS. Visual field sensitivity losses suggest neural abnormalities in early stage diabetic eye disease and the pattern of the sensitivity losses differed depending on the adaptation conditions. Chromatic perimetry may be useful for subtyping individuals who have mild or no diabetic retinopathy and for better understanding their neural dysfunction.

Keywords: diabetic retinopathy (DR), visual field perimetry, visual sensitivity, neural dysfunction

Diabetic retinopathy (DR) is one of the leading causes of vision loss worldwide.^{1–3} Currently, diagnosis and staging of DR are based on abnormalities of the retinal vasculature,⁴ but there is accumulating evidence that retinal neurodegeneration may precede the clinically apparent vascular changes. For example, optical coherence tomography (OCT) studies have reported inner retinal thinning in individuals who have diabetes mellitus (DM) and mild or no DR.^{5–16} Neurodegeneration in early stage DR has also been associated with functional abnormalities, including psychophysical contrast sensitivity losses,^{17,18} as well as electrophysiological¹⁹ and pupillometric^{20,21} abnormalities. Visual field perimetry, a technique most commonly used in glaucoma, also has a long history of application in diabetes. Early work identified visual field sensitivity losses, even in eyes without clinically apparent DR.²² However, more recent work using standard automated perimetry (SAP) in early stage DR has been equivocal: several SAP studies have shown reductions in field sensitivity,^{8,23–25} but the reductions did not necessarily achieve statistical significance.^{8,23} As reviewed elsewhere,²⁶ the relatively poor sensitivity of SAP in early stage DR has prompted the use of alternative perimetry procedures (e.g. short-wavelength automated

perimetry and frequency doubling perimetry) for studying field abnormalities.

Sensitivity loss in individuals with diabetes has typically been measured under photopic conditions (i.e. “white-on-white” SAP) or under mesopic conditions using microperimetry.²⁷ Visual field sensitivity under dark-adapted conditions, in which performance is mediated by the rod pathway, may provide a more sensitive measure of visual dysfunction. That is, under dark-adapted conditions, there is high metabolic demand of the rod photoreceptors, which may result in hypoxia in the diabetic retina.²⁸ However, sensitivity losses under photopic conditions assessed with white light and under scotopic conditions assessed with blue light were reported to be approximately similar in individuals with diabetes.²⁹ To date, sensitivity losses under photopic and scotopic conditions assessed with the same stimulus have not been compared in individuals with diabetes, nor has the pattern of field loss (e.g. diffuse versus localized) been compared under photopic and scotopic conditions.

We have recently described an approach for measuring dark-adapted thresholds using a commercially available Octopus 900 field perimeter (Haag-Streit, Koeniz, Switzerland)^{30,31} that can be adapted to measure light-adapted

thresholds as well. An advantage of this approach is that insight into the pathway mediating performance across the field can be obtained by measuring and comparing sensitivity for red (long-wavelength) and blue (short-wavelength) stimuli. As discussed in detail elsewhere,³² differences in rod and cone spectral sensitivity predict that sensitivity for red and blue stimuli will differ considerably (e.g. 100 times, depending on stimulus wavelength) when measurements are mediated by the rod pathway, but will be approximately equivalent when measurements are mediated by the cone pathway. This chromatic perimetry approach has been applied extensively to study sensitivity in patients with retinitis pigmentosa,^{32–34} but has yet to be performed in individuals with DR.

In the present study, sensitivity was measured across the visual field under dark- and light-adapted conditions using long- and short-wavelength stimuli in patients with diabetes who had either no clinically apparent diabetic retinopathy (NDR) or mild nonproliferative diabetic retinopathy (MDR). This permitted determining the extent to which rod- and cone-pathway function was affected in these individuals. In addition, advanced field analytics were used to quantify the nature of the field loss (diffuse versus localized) under dark- and light-adapted conditions. Thus, we sought to provide a comprehensive analysis of sensitivity across the visual field in early stage DR.

METHODS

Subjects

This study followed the tenants of the Declaration of Helsinki and institutional review board approval was obtained at the University of Illinois at Chicago. The experiments were undertaken with the understanding and written consent of each subject. Thirty-four subjects diagnosed with type 2 DM were recruited from the Retina and General Eye Clinics of the University of Illinois at Chicago, Department of Ophthalmology and Visual Sciences. Each subject was examined by a retina specialist and medical histories were obtained from their records. The stage of NPDR was graded clinically according to the Early Treatment of Diabetic Retinopathy Study (ETDRS) scale⁴ and the subjects were classified as diabetic with no apparent DR (NDR; $N = 17$) or diabetic with mild NPDR (MDR; $N = 17$) based on fundus examination. Subjects classified as MDR had minimal retinal vascular abnormalities including microaneurysms, hard exudates, and cotton-wool spots (equivalent to ETDRS⁴ level 35 or less). No subject had other ocular or systemic diseases known to affect the retina. Exclusion criteria included sickle cell disease, retinal vascular occlusions, age-related macular degeneration, glaucoma, and high myopia (more than 6 diopters). Lens status was graded by slit lamp examination using a clinical scale that ranged from

clear to 4+. Subjects with more than mild (2+) nuclear sclerotic, posterior subcapsular, or cortical lens opacities were excluded. Most NDR subjects ($N = 10$) had clear lenses or trace nuclear sclerotic cataract; one NDR subject had a 2+ nuclear sclerotic cataract. Likewise, MDR subjects ranged from clear/trace ($N = 6$) to 2+ nuclear sclerotic cataract ($N = 2$). None of the subjects had a history of diabetic macular edema. Subject characteristics including age, sex, best-corrected visual acuity, estimated diabetes duration, and HbA1c percentage are provided in the Table. Visual acuity for the NDR group was slightly (0.07 log MAR), but significantly, better than that of the MDR group ($t = 2.66$, $P = 0.01$). The duration of diabetes was significantly shorter for the NDR group compared to the MDR group ($t = 3.49$, $P = 0.002$). There was no significant difference in HbA1c between the NDR and MDR groups ($t = 1.13$, $P = 0.27$).

Fifteen non-diabetic control subjects also participated. The same exclusion criteria discussed above were also applied to the control subjects (i.e. free of systemic disease known to affect the retina, no prior ocular surgery with the exception of non-complicated cataract removal, and no more than moderate myopia). The control subjects had best-corrected visual acuity of 0.1 log MAR (approximately 20/25 Snellen equivalent) or better. A one-way analysis of variance indicated no significant difference in mean age among the control and DM groups ($F = 0.32$, $P = 0.73$). Of note, three of the control subjects had prior experience with perimetry testing; none of the DM subjects reported prior experience with perimetry.

Apparatus, Stimuli, Procedure, and Analysis

A commercially available Octopus 900 Pro perimeter (Haag-Streit, Bern, Switzerland) was used for stimulus generation and presentation. The test stimuli were blue (449 nm peak wavelength) and red (610 nm peak wavelength) spots of light that subtended 0.43 degrees (Goldmann III). Stimulus luminance was measured with a PhotoResearch Spectra Scan PR740 spectroradiometer and defined in photopic cd/m^2 . The test stimuli were presented for 100 ms at 15 different locations along the horizontal meridian of the visual field. Sensitivity was finely sampled in the central retina and more sparsely sampled in the periphery (test locations were: 0, ± 2 degrees, ± 5 degrees, ± 10 degrees, -15 degrees, ± 20 degrees, ± 30 degrees, ± 45 degrees, and $+60$ degrees; positive values represent measurements from the nasal retina, whereas negative values represent measurements from the temporal retina). To facilitate descriptions of the data, the 15 locations were grouped into 4 regions: foveal (0 degrees), parafoveal field (2 degrees), perifoveal field (5 degrees–10 degrees), and peripheral field (10 degrees–60 degrees). The stimuli were presented either in the dark (no background) or against an achromatic 10 cd/m^2 background.

Although training was not provided, the test procedure was explained in detail to each subject and the need to

TABLE. Subject Characteristics

	Control ($N = 15$)	No DR ($N = 17$)	Mild NPDR ($N = 17$)
Age, y	52.1 \pm 9.4	54.2 \pm 6.6	54.1 \pm 8.2
Sex	4 M and 11 F	5 M and 12 F	8 M and 9 F
Log MAR acuity	0.00 \pm 0.07	0.05 \pm 0.06	0.12 \pm 0.08
Disease duration, y		6.0 \pm 4.8	12.4 \pm 5.7
HbA1c, %		7.5 \pm 1.3	8.4 \pm 2.6

y is years; M is male and F is female; MAR is minimum angle of resolution; HbA1c is glycated hemoglobin.

maintain correct fixation throughout the test was emphasized. The Octopus software monitors fixation and pauses the test in the event of large eye movements, but the stimulus location is not adjusted in real time as in microperimetry. Following the instructions, sensitivity was measured under light-adapted conditions. Following the light-adapted testing, subjects were dark-adapted for 30 minutes before performing the dark-adapted measurements. Appropriate refractive correction was used for test targets presented within the central 20 degrees (radius) of the visual field and removed for targets presented more peripherally. All testing was performed monocularly, with the fellow eye patched. For the control subjects, measurements were obtained from the right eyes, whereas the eye with the best visual acuity was tested for the diabetic subjects (the right eye was tested for 25/34 DM subjects who had eyes of equal acuity). Data obtained from the left eye were replotted in right eye format to facilitate comparisons. Sensitivity was measured using the Octopus EyeSuite 4-2-1 staircase procedure. These measurements (dB attenuation) were exported and a custom-written MATLAB script was used to extract the sensitivity values for the corresponding field locations.

Cumulative defect curves (CDCs) were created to determine whether the pattern of sensitivity loss across the field was diffuse (i.e. all locations of the field similarly affected) or localized (certain areas of the field affected more than others). Importantly, CDCs provide a useful approach that can overcome the limitation of intersubject differences in the location of sensitivity loss.³⁵ CDCs rank sensitivity loss across the visual field (best performing area to worst performing area). To construct these curves, sensitivity for each subject for each of the 15 field locations was subtracted from the corresponding mean control sensitivity value at the corresponding location. The sensitivity loss from normal (“defect”) is plotted according to the defect depth, from smallest defect to largest defect. Supplementary Figure S1 shows hypothetical CDCs from a normal subject and predicted outcomes that could be observed for the DM subjects. For quantification of diffuse and localized losses, diffuse loss was defined as the mean defect across the 3 to 5 best performing areas of the field, whereas localized loss was defined as the mean defect across the 12 to 14 worst performing areas of the field. The largest and smallest index values were not included in the analysis to avoid false negatives and false positives (i.e. the worst performing area [index 15] could be influenced by blinks/attention lapses).³⁵ The diffuse loss (mean sensitivity loss for index values 3, 4, and 5) was subtracted from the localized loss (mean sensitivity loss for index values 12, 13, and 14) to correct for the overall downward shift of the CDC, providing a better measure of the localized defect.

Although CDCs permit comparing the pattern of sensitivity loss (diffuse/localized) among subjects with different locations of sensitivity loss, the approach has two limitations. First, diffuse/localized losses can only be assessed at the “field level” and cannot be related back to a specific field location. Second, removing spatial information can limit assessment of the underlying physiology (i.e. rod- versus cone-mediated sensitivity losses).

RESULTS

Figure 1 plots mean log sensitivity (\pm SEM) measured along the horizontal meridian for the control subjects (black triangles), NDR subjects (green circles), and MDR subjects (red

squares). Data obtained under light-adapted conditions with red (A) and blue (B) stimuli are shown in the top row, and under dark-adapted conditions for red (C) and blue (D) stimuli in the bottom row. Under light-adapted conditions, log sensitivity for the long- and short-wavelength stimuli were similar, and sensitivity increased from the far periphery toward the fovea for all subjects. Overall, sensitivities were generally reduced throughout the field area tested for the NDR and MDR groups compared with the controls. For the NDR subjects, the mean red (-0.58 log) and blue (-0.41 log) sensitivities averaged across the field were similarly reduced in comparison to the mean control red (-0.40 log) and blue (-0.18 log) sensitivities (0.18 and 0.23 log unit reductions for the red and blue stimuli, respectively). For the MDR subjects, the mean red sensitivity averaged across the field was -0.60 log and the mean blue sensitivity was -0.68 log. Relative to the controls, sensitivity was more reduced for the blue stimulus (0.50 log units) than for the red stimulus (0.23 log units). Sensitivities for the three subject groups were compared using repeated measures analysis of variance (ANOVA) with subject group (control, NDR, and MDR) and field location included as main effects. The ANOVA indicated significant differences among the groups measured with both the red ($F = 3.86$, $P = 0.03$) and blue ($F = 11.20$, $P < 0.001$) stimuli. Differences in sensitivity between the control group and the two diabetic groups for each retinal location were compared with Holm-Sidak pairwise comparisons, with the results presented in Supplementary Table S1.

The dark-adapted red (see Fig. 1C) and blue (see Fig. 1D) sensitivity profiles differed considerably from those obtained under light-adapted conditions for all subject groups. That is, dark-adapted sensitivity for the red stimulus increased gradually from the periphery toward the fovea, forming a shallow inverted U-shape, whereas dark-adapted sensitivity for the blue stimulus was lowest at the fovea and increased sharply in the parafovea. Overall, dark-adapted sensitivities were reduced for the DM groups compared with the controls. Specifically, sensitivity for the dark-adapted red and blue stimuli were reduced by 0.18 and 0.19 log units for the NDR subjects, respectively, and by 0.36 and 0.52 log units for the MDR subjects, respectively. Repeated measures ANOVA indicated significant differences among the groups measured with both the dark-adapted red ($F = 3.47$, $P = 0.04$) and blue ($F = 3.75$, $P = 0.03$) stimuli. Differences in sensitivity between the control group and the two diabetic groups for each retinal location were compared with Holm-Sidak pairwise comparisons, with the results presented in Supplementary Table S1.

As discussed in detail elsewhere,³² comparison of sensitivity values measured for red- and blue stimuli can be used to infer the visual pathway (rod versus cone) mediating sensitivity. Supplementary Figure S2 shows the difference between red and blue sensitivity under dark- and light-adapted conditions for the three subject groups. Similar sensitivities were observed for the red and blue stimuli across the field, indicating that sensitivity is mediated by the cone-pathway at all locations for both stimulus colors under light-adapted conditions.³² In contrast, under dark-adapted conditions, red and blue sensitivity values were similar at the fovea and differed by approximately 1.8 log units in the periphery. Similar sensitivities for the red and blue stimuli at the fovea indicate cone-pathway mediation, whereas the 1.8 log unit difference in the periphery is consistent with rod pathway mediation.

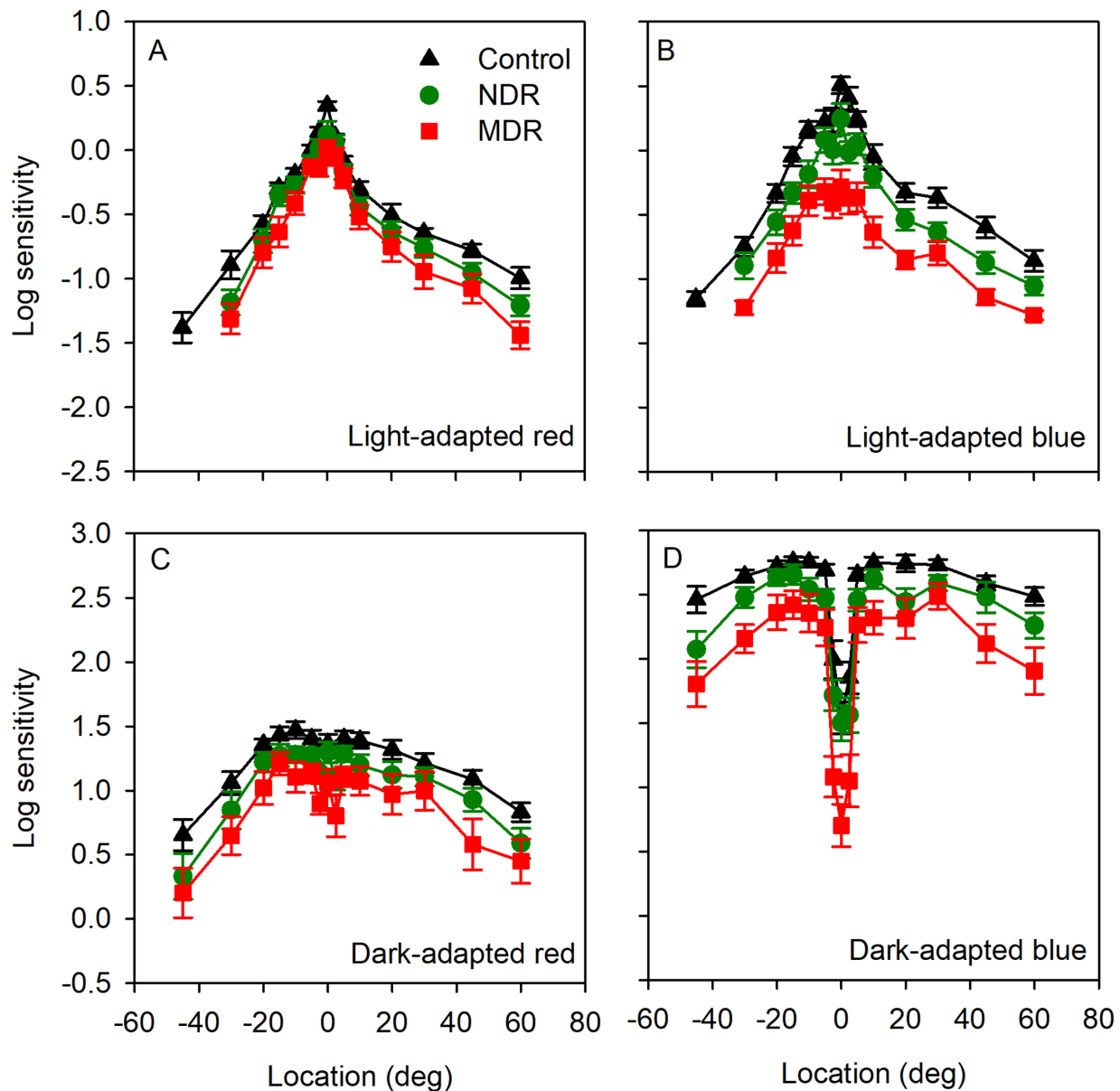


FIGURE 1. Mean (\pm SEM) log sensitivity as a function of retinal location for the control subjects (*black triangles*), NDR subjects (*green circles*), and MDR subjects (*red squares*). Sensitivity is defined as $1/\text{threshold}$ (cd/m^2). Data were obtained under light-adapted conditions with the red stimulus (**A**), light-adapted conditions with the blue stimulus (**B**), dark-adapted conditions with the red stimulus (**C**), dark-adapted conditions with the blue stimulus (**D**). Negative x-axis values represent measurements from the temporal retina, whereas positive x-axis values represent measurements from the nasal retina. For the most peripheral temporal retina location tested (-45 degrees) under light-adapted conditions, the perimeter could not produce sufficient light to measure sensitivity for the NDR and MDR subjects (ceiling effect); data points at -45 degrees have been omitted from the plots in **A** and **B**.

The mean data shown in [Figure 1](#) suggest that sensitivity is uniformly reduced across the visual field in the NDR and MDR groups, relative to the control group. Although this is the case for the group averages, individual subjects differed considerably in the spatial pattern of sensitivity loss. An example of two MDR subjects, both tested under light-adapted conditions with the red stimulus, is provided in [Supplementary Figure S3](#). This figure shows clear differences in the locations of sensitivity loss for these two subjects. To account for differences in the location of field sensitivity loss among subjects, CDCs were constructed and are presented in [Figure 2](#).

[Figure 2](#) shows the mean CDCs (\pm 95% confidence intervals) for the NDR (green circles) and MDR (red squares)

subjects, compared to the control range (the gray region represents the 95% confidence interval of the controls). Under light-adapted conditions, the CDCs for the NDR and MDR subjects are generally shifted downward, indicating a diffuse pattern of sensitivity loss for the red (see [Fig. 2A](#)) and blue (see [Fig. 2B](#)) stimuli. Under dark-adapted conditions, the sensitivity loss was considerably greater for the poorest performing areas of the field, consistent with localized losses for both DM groups. Note, however, that the curves are shifted downward somewhat, particularly for the MDR subjects assessed with the blue stimulus.

The localized and diffuse sensitivity losses were quantified and are displayed in [Figure 3](#). The colored boxes represent the normal control data for the red stimulus

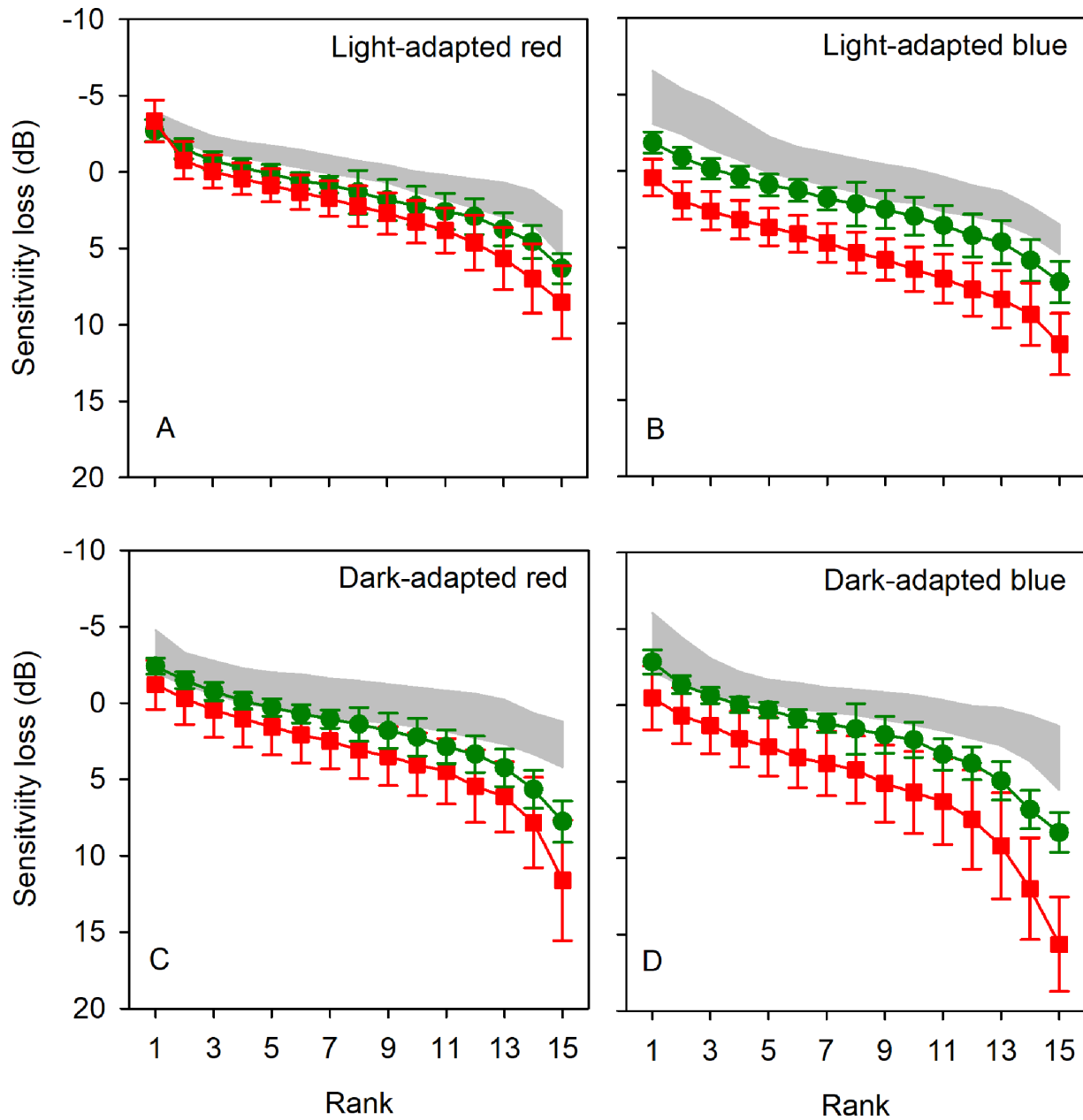


FIGURE 2. Mean ($\pm 95\%$ confidence interval) CDCs are shown for the NDR (green circles) and MDR (red squares) subjects in comparison to the 95% confidence interval of the controls (gray region). Data were obtained under light-adapted conditions with the red stimulus (A), light-adapted conditions with the blue stimulus (B), dark-adapted conditions with the red stimulus (C), dark-adapted conditions with the blue stimulus (D).

(mean ± 2 SD; red box) and blue stimulus (mean ± 2 SD; blue box); each symbol represents an individual DM subject (NDR = green circles and MDR = red squares). The control range was calculated by subtracting each control sensitivity value from the mean control group sensitivity value. Under light-adapted conditions, diffuse sensitivity losses are apparent for DM subjects assessed with both red ($N = 9$ NDR and $N = 9$ MDR) and blue ($N = 4$ NDR and $N = 8$ MDR) stimuli (Fig. 4A). One way ANOVA with Holm-Sidak multiple comparisons indicated significant diffuse light-adapted field losses for both the NDR and MDR subjects, assessed with both the red and blue stimuli ($t > 2.52$, $P < 0.02$; see asterisks in Fig. 4A). By contrast, Figure 4B shows that localized light-adapted losses were generally small and

only reached statistical significance for the MDR subjects assessed with the red stimulus ($t = 3.26$, $P = 0.004$). A nearly opposite pattern was observed for the dark-adapted measurements, in that the losses were primarily localized in nature. Specifically, Figure 3C shows that diffuse dark-adapted losses were generally small and only reached statistical significance for the MDR subjects assessed with the blue stimulus ($t = 3.67$, $P = 0.001$). The dark-adapted localized losses (see Fig. 3D) were large and statistically significant for both groups assessed with both colors (all $t > 2.40$, $P < 0.02$). For the red stimulus, 8 NDR and 11 MDR subjects were below the normal range, whereas for the blue stimulus, 7 NDR and 12 MDR subjects were below the normal range.

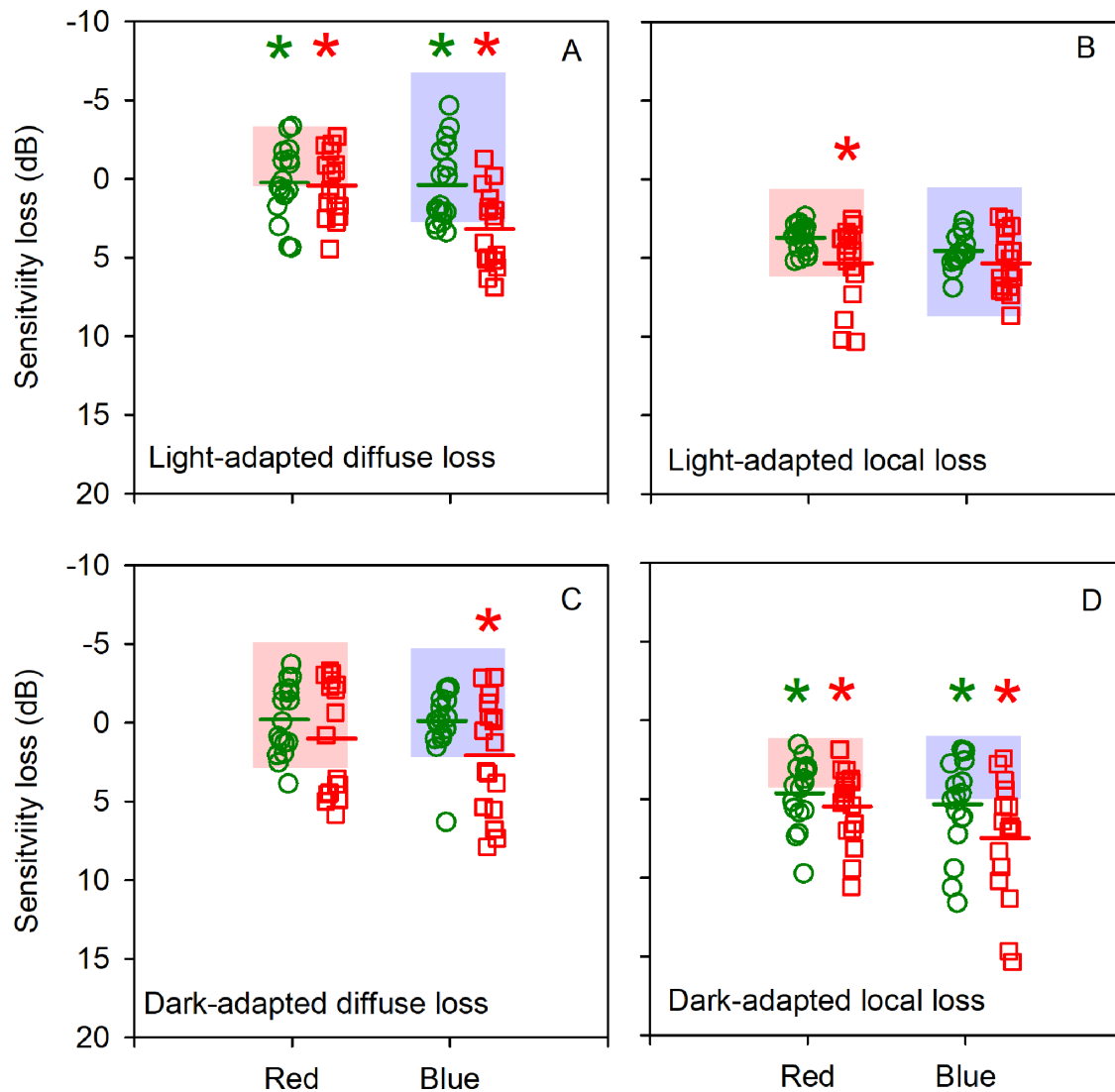


FIGURE 3. Diffuse and localized sensitivity losses are quantified from Figure 2 for each DM subject compared to the normal range (mean ± 2 SD; shaded regions). Diffuse losses measured under light-adapted conditions with the red (*left* data set) and blue (*right* data set) stimuli are shown in (A). Localized losses measured under light-adapted conditions with the red (*left* data set) and blue (*right* data set) stimuli are shown in (B). Panels (C) and (D) show the dark-adapted diffuse and localized losses, with other conventions as in panels A and B. Horizontal bars for each dataset represent the group means.

The diffuse and localized sensitivity losses were compared with clinical characteristics for the NDR and MDR groups. For the NDR group, neither age (all r between -0.46 and 0.10 , all $P > 0.06$) nor diabetes duration (all r between -0.47 and 0.24 , all $P > 0.07$) were correlated significantly with the sensitivity loss values under dark- or light-adapted conditions. HbA1c was modestly correlated with localized sensitivity loss for the light-adapted red condition ($r = -0.63$, $P = 0.01$), but this was not considered statistically significant after correction for multiple comparisons. For all other conditions, HbA1c was poorly correlated with sensitivity loss (all r between -0.41 and 0.33 , all $P > 0.23$). For the MDR group, age was weakly correlated with sensitivity loss (r between -0.04 and -0.69 , all P between 0.89 and 0.02), but this was not considered statistically significant after correction for multiple comparisons. There were also no significant correlations between diabetes duration and sensitivity loss (all r between -0.32 and 0.13 , all $P > 0.22$) or between HbA1c and sensitivity loss (all r between -0.48

and 0.04 , all $P > 0.07$). Thus, there were no significant correlations between the patients' clinical characteristics and the visual field sensitivity losses for either diabetic group.

Figure 4 highlights the usefulness of considering the extent of neural dysfunction in the classification of diabetic retinal disease. The left panel classifies the 34 diabetic subjects according to traditional clinical criteria: DR stage and extent of macular edema. All DM subjects recruited for this study had NDR (green circles) or MDR (red squares) with no edema. Consequently, these subjects cluster along the x-axis in two groups, suggesting homogeneity within the groups. The right panel adds a third axis that represents the extent of neural dysfunction defined by the localized dark-adapted blue sensitivity loss (from Fig. 3D). It is clear that there is marked heterogeneity of neural dysfunction within the NDR and MDR groups, with individuals within each group ranging from normal neural function (less than 3 dB loss; gray region) to considerable neural dysfunction (red region). Although the DM subjects are similar in

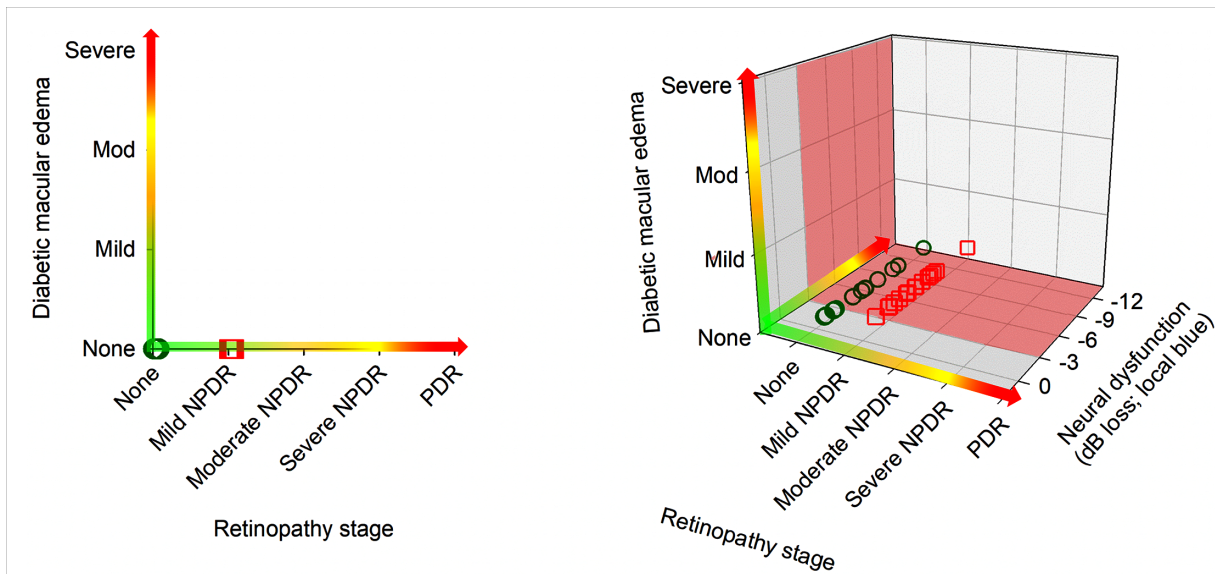


FIGURE 4. The utility of measuring neural dysfunction to sub-classify DM subjects is illustrated. The left panel presents the standard classification criteria (diabetic macular edema and retinopathy stage); all subjects cluster along the x-axis into two groups. The right panel adds a z-axis that includes the extent of neural dysfunction as assessed by localized blue sensitivity loss (from Fig. 3). The red region represents abnormal neural function, defined as a 3 dB or greater loss of sensitivity.

their retinopathy grade and edema characteristics, they differ considerably in their extent of neural dysfunction.

DISCUSSION

This study evaluated the nature and extent of visual field sensitivity loss, assessed by chromatic light- and dark-adapted perimetry, in subjects with NDR and MDR. The primary findings of the study are: (1) two-color perimetry can be used to determine whether the rod- or cone-pathway mediated sensitivity for each retinal location tested. The pathway mediating sensitivity did not differ for the control and DM subjects. (2) Sensitivity is reduced, on average, for NDR and MDR subjects under light- and dark-adapted conditions. (3) The retinal locations of the sensitivity losses differ among individuals. (4) Advanced field analytics indicate that field sensitivity losses tend to be diffuse in nature under light-adapted conditions and tend to be localized in nature under dark-adapted conditions.

Sensitivity was significantly reduced for both DM groups under light- and dark-adapted conditions. For the NDR group, sensitivity was reduced similarly under all conditions (approximately 1.6 times). In contrast, the MDR subjects were more reduced for the blue stimulus (approximately 3.2 times) than for the red stimulus (approximately 2.0 times). The greater loss of blue sensitivity compared to red sensitivity is consistent with tritan defects reported previously in DM.^{26,36} We initially hypothesized that rod pathway function would be more affected than cone pathway function, but this hypothesis was not supported by the data. Sensitivity was similarly reduced under light- and dark-adapted conditions for the NDR (approximately 1.5 times) and MDR (approximately 2.5 times) groups. This finding may suggest that rod and cone photoreceptors are equally affected in DM. Alternatively, diabetes may affect common downstream sites (bipolar and/or retinal ganglion cells), which would more parsimoniously account for the similar sensitivity losses under photopic and scotopic conditions.

The average (\pm SEM) light-adapted mean deviations for the NDR (-2.1 ± 0.6 dB) and MDR (-4.0 ± 0.7 dB) subjects are generally consistent with those reported previously for white on white (photopic) SAP, which ranged from -0.9 dB to -1.4 dB for NDR subjects and -1.8 dB to -4.1 dB for MDR subjects.^{8,24,29,37} Likewise, the average dark-adapted mean deviations for the NDR (-1.9 ± 0.7 dB) and MDR (-4.5 ± 1.0 dB) subjects are generally consistent with those reported previously²⁹ for dark-adapted blue SAP for NDR (-0.5 dB) and MDR (-4.1 dB) subjects. We are not aware of previous reports of dark-adapted red sensitivity measurements in diabetic subjects that would permit comparisons to the present data set.

Although the group average sensitivity losses were generally uniform across the horizontal meridian of the field, this was not necessarily the case for individual subjects. Indeed, there was considerable intersubject variation in the location of the threshold elevations (see Supplementary Fig. S3). Because of this, simple averaging and calculation of mean deviation is not ideal for understanding the nature of the field loss; more advanced analyses are required. Consequently, CDCs were constructed to determine for each subject whether the field loss was diffuse or localized. Under light-adapted conditions in which the cone-pathway mediated sensitivity, the field loss was diffuse: the best-performing area of the field was as affected as the worst-performing area. Interestingly, under dark-adapted conditions in which the rod-pathway mediated sensitivity, the opposite pattern was found: field loss was localized, wherein the best-performing area of the field was much less affected than the worst-performing area. This may suggest that diabetes results in uniform loss of cone function and patchy/localized loss of rod function. Alternatively, diabetes may similarly affect the rod and cone photoreceptors, but downstream signaling (bipolar/retinal ganglion cells) may be differently affected by the adaptation conditions. Adaptation level (i.e. scotopic, mesopic, and photopic) is known to affect spatial summation, with receptive field size

growing as illumination is reduced.^{38,39} This may make localized field loss more detectable under dark-adapted conditions. Although this is speculative and the explanation for the different patterns of field loss under light- and dark-adapted conditions is uncertain, it does appear that assessment of localized field loss under dark-adapted conditions is a sensitive marker for the effects of DM on neural function. It is also important to consider that all measurements in the present study were obtained along the horizontal meridian of the visual field. Consequently, we cannot determine whether similar patterns of sensitivity loss are present at other visual field locations.

Individuals with diabetes often develop early cataract^{40,41} that would result in diffuse sensitivity loss, particularly for blue stimuli. As noted above, blue sensitivity was, on average, more reduced than red sensitivity for the MDR group. However, it is unlikely that cataract can explain the field sensitivity losses. First, subjects with more than mild cataract were not recruited for this study. Second, similar diffuse losses were observed with the red and blue stimuli under light-adapted conditions. If early cataracts underlie the sensitivity losses, it would be expected that the diffuse blue loss would exceed the diffuse red loss. Nevertheless, potential optical abnormalities should be considered in the interpretation of psychophysical sensitivity data.

The present sample of diabetic subjects was selected to be generally homogeneous in terms of their clinical characteristics: subjects had either no DR or mild DR and none had diabetic macular edema. Of note, clinical characteristics were defined by fundus examination only; fundus photography, fluorescein angiography, and OCT angiography were not performed, which may have limited our ability to identify subtle vascular lesions. Despite similar clinical characteristics, these subjects differed considerably in the extent of neural dysfunction (illustrated in Fig. 4). For example, localized field loss under dark-adapted conditions ranged from normal to more than 10 dB below normal. Given the intersubject differences, localized field loss may be a useful measure for subtyping patients for future clinical trials that target early stage DR. That is, individuals who have neural dysfunction, assessed with chromatic perimetry, may show a greater benefit of neuroprotective therapeutics as compared to individuals who have normal neural function. The value of chromatic perimetry for patient selection and outcome assessment remains to be determined in longitudinal trials.

In summary, individuals who have mild or no DR can have considerable field sensitivity losses that are typically diffuse in nature under light-adapted conditions and localized under dark-adapted conditions. Given the localized nature of the field loss under dark-adapted conditions, mean deviation is not an optimal index of sensitivity. The combination of chromatic perimetry and advanced field analytics (i.e. cumulative defect curve analysis) may be useful for clinical trials in early stage DR and for understanding fundamental pathophysiological mechanisms in these patients. These findings support previous proposals^{42,43} to expand the classification of diabetic eye disease to include neural abnormalities and provide one approach to define neural dysfunction in these individuals.

Acknowledgments

Supported by National Institutes of Health research grants R01EY026004 (J.M.) and P30EY001792 (core grant), and an unrestricted departmental grant from Research to Prevent Blind-

ness. The funding organizations had no role in the design or conduct of this research.

Disclosure: **J.J. McAnany**, None; **J.C. Park**, None; **J.I. Lim**, None

References

- Klein BE. Overview of epidemiologic studies of diabetic retinopathy. *Ophthalmic Epidemiol.* 2007;14:179–183.
- Lee R, Wong TY, Sabanayagam C. Epidemiology of diabetic retinopathy, diabetic macular edema and related vision loss. *Eye Vis (Lond).* 2015;2:17.
- Yau JW, Rogers SL, Kawasaki R, et al. Global prevalence and major risk factors of diabetic retinopathy. *Diabetes Care.* 2012;35:556–564.
- Davis MD, Fisher MR, Gangnon RE, et al. Risk factors for high-risk proliferative diabetic retinopathy and severe visual loss: Early Treatment Diabetic Retinopathy Study Report #18. *Invest Ophthalmol Vis Sci.* 1998;39:233–252.
- Chhablani J, Sharma A, Goud A, et al. Neurodegeneration in type 2 diabetes: Evidence from spectral-domain optical coherence tomography. *Invest Ophthalmol Vis Sci.* 2015;56:6333–6338.
- Carpineto P, Toto L, Aloia R, et al. Neuroretinal alterations in the early stages of diabetic retinopathy in patients with type 2 diabetes mellitus. *Eye (Lond).* 2016;30:673–679.
- Gundogan FC, Akay F, Uzun S, Yolcu U, Cagiltay E, Toyran S. Early Neurodegeneration of the Inner Retinal Layers in Type 1 Diabetes Mellitus. *Ophthalmologica.* 2016;235:125–132.
- Joltikov KA, de Castro VM, Davila JR, et al. Multidimensional functional and structural evaluation reveals neuroretinal impairment in early diabetic retinopathy. *Invest Ophthalmol Vis Sci.* 2017;58: BIO277–BIO290.
- Sohn EH, van Dijk HW, Jiao C, et al. Retinal neurodegeneration may precede microvascular changes characteristic of diabetic retinopathy in diabetes mellitus. *Proc Natl Acad Sci U S A.* 2016;113:E2655–E2664.
- van Dijk HW, Kok PH, Garvin M, et al. Selective loss of inner retinal layer thickness in type 1 diabetic patients with minimal diabetic retinopathy. *Invest Ophthalmol Vis Sci.* 2009;50:3404–3409.
- van Dijk HW, Verbraak FD, Kok PH, et al. Decreased retinal ganglion cell layer thickness in patients with type 1 diabetes. *Invest Ophthalmol Vis Sci.* 2010;51:3660–3665.
- van Dijk HW, Verbraak FD, Kok PH, et al. Early neurodegeneration in the retina of type 2 diabetic patients. *Invest Ophthalmol Vis Sci.* 2012;53:2715–2719.
- Vujosevic S, Miden E. Retinal layers changes in human preclinical and early clinical diabetic retinopathy support early retinal neuronal and Muller cells alterations. *J Diabetes Res.* 2013;2013:905058.
- Bialosterski C, van Velthoven ME, Michels RP, Schlingemann RO, DeVries JH, Verbraak FD. Decreased optical coherence tomography-measured pericentral retinal thickness in patients with diabetes mellitus type 1 with minimal diabetic retinopathy. *Br J Ophthalmol.* 2007;91:1135–1138.
- Rodrigues EB, Urias MG, Penha FM, et al. Diabetes induces changes in neuroretina before retinal vessels: A spectral-domain optical coherence tomography study. *Int J Retina Vitreous.* 2015;1:4.
- Park JC, Chen YF, Liu M, Liu K, McAnany JJ. Structural and functional abnormalities in early-stage diabetic retinopathy. *Curr Eye Res.* 2020;45:975–985.
- McAnany JJ, Park JC. Reduced contrast sensitivity is associated with elevated equivalent intrinsic noise in type 2 diabetics who have mild or no retinopathy. *Invest Ophthalmol Vis Sci.* 2018;59:2652–2658.

18. Stavrou EP, Wood JM. Letter contrast sensitivity changes in early diabetic retinopathy. *Clin Exp Optom*. 2003;86:152–156.
19. McAnany JJ, Persidina OS, Park JC. Clinical electroretinography in diabetic retinopathy: A review. *Surv Ophthalmol*. 2022;67(3):712–722.
20. Feigl B, Zele AJ, Fader SM, et al. The post-illumination pupil response of melanopsin-expressing intrinsically photosensitive retinal ganglion cells in diabetes. *Acta Ophthalmol*. 2012;90:e230–e234.
21. Park JC, Chen YF, Blair NP, et al. Pupillary responses in non-proliferative diabetic retinopathy. *Sci Rep*. 2017;7:44987.
22. Roth JA. Central visual field in diabetes. *Br J Ophthalmol*. 1969;53:16–25.
23. Lobefalo L, Verrotti A, Mastropasqua L, et al. Blue-on-yellow and achromatic perimetry in diabetic children without retinopathy. *Diabetes Care*. 1998;21:2003–2006.
24. Parravano M, Oddone F, Mineo D, et al. The role of Humphrey Matrix testing in the early diagnosis of retinopathy in type 1 diabetes. *Br J Ophthalmol*. 2008;92:1656–1660.
25. Trick GL, Trick LR, Kilo C. Visual field defects in patients with insulin-dependent and noninsulin-dependent diabetes. *Ophthalmology*. 1990;97:475–482.
26. Chen XD, Gardner TW. A critical review: Psychophysical assessments of diabetic retinopathy. *Surv Ophthalmol*. 2021;66:213–230.
27. Midena E, Vujosevic S. Microperimetry in diabetic retinopathy. *Saudi J Ophthalmol*. 2011;25:131–135.
28. Kern TS, Berkowitz BA. Photoreceptors in diabetic retinopathy. *J Diabetes Investig*. 2015;6:371–380.
29. Jackson GR, Scott IU, Quillen DA, Walter LE, Gardner TW. Inner retinal visual dysfunction is a sensitive marker of non-proliferative diabetic retinopathy. *Br J Ophthalmol*. 2012;96:699–703.
30. Igelman AD, Ku C, Mershon S, et al. Effect of pharmacological pupil dilation on dark-adapted perimetric sensitivity in healthy subjects using an octopus 900 perimeter. *Transl Vis Sci Technol*. 2021;10:18.
31. Igelman AD, Park JC, Hyde RA, et al. Two-color dark-adapted perimetry implemented with a commercially available perimeter to characterize rod-pathway sensitivity. *Ophthalmic Surg Lasers Imaging Retina*. 2022;53:692–696.
32. Massof RW, Finkelstein D. Two forms of autosomal dominant primary retinitis pigmentosa. *Doc Ophthalmol*. 1981;51:289–346.
33. Apushkin MA, Fishman GA, Alexander KR, Shahidi M. Retinal thickness and visual thresholds measured in patients with retinitis pigmentosa. *Retina*. 2007;27:349–357.
34. Jacobson SG, Voigt WJ, Parel JM, et al. Automated light- and dark-adapted perimetry for evaluating retinitis pigmentosa. *Ophthalmology*. 1986;93:1604–1611.
35. Bebie H, Flammer J, Bebie T. The cumulative defect curve: Separation of local and diffuse components of visual field damage. *Graefes Arch Clin Exp Ophthalmol*. 1989;27:9–12.
36. Wolff BE, Bearnse MA, Schneck ME, et al. Color vision and neuroretinal function in diabetes. *Doc Ophthalmol*. 2015;130:131–139.
37. Zico OA, El-Shazly AA, Abdel-Hamid Ahmed EE. Short wavelength automated perimetry can detect visual field changes in diabetic patients without retinopathy. *Indian J Ophthalmol*. 2014;62:383–387.
38. Cornsweet TN, Yellott JJ. Intensity-dependent spatial summation. *J Opt Soc Am A*. 1985;2:1769–1786.
39. Barlow HB. Temporal and spatial summation in human vision at different background intensities. *J Physiol*. 1958;141:337–350.
40. Javadi MA, Zarei-Ghanavati S. Cataracts in diabetic patients: A review article. *J Ophthalmic Vis Res*. 2008;3:52–65.
41. Klein BE, Klein R, Moss SE. Incidence of cataract surgery in the Wisconsin Epidemiologic Study of Diabetic Retinopathy. *Am J Ophthalmol*. 1995;119:295–300.
42. Abramoff MD, Fort PE, Han IC, Jayasundera KT, Sohn EH, Gardner TW. Approach for a clinically useful comprehensive classification of vascular and neural aspects of diabetic retinal disease. *Invest Ophthalmol Vis Sci*. 2018;59:519–527.
43. Sun JK, Aiello LP, Abramoff MD, et al. Updating the staging system for diabetic retinal disease. *Ophthalmology*. 2021;128:490–493.